THE EUROPEAN
PHYSICAL JOURNAL B

Frequency-dependent fluctuational conductivity above T_c in anisotropic superconductors: effects of a short wavelength cutoff

E. Silva[a]

Dipartimento di Fisica "E. Amaldi" and Unità INFM, Università di Roma Tre, Via della Vasca Navale 84, 00146 Roma, Italy

Abstract. We discuss the excess conductivity at nonzero frequencies in a superconductor above T_c within the Gaussian approximation. We focus the attention on the temperature range not too close to T_c: within a time-dependent Ginzburg-Landau formulation, we phenomenologically introduce a short wavelength cutoff (of the order of the inverse coherence length) in the fluctuational spectrum to suppress high momentum modes. We treat the general cases of thin wires, anisotropic thin films and anisotropic bulk samples. We obtain in all cases explicit expressions for the finite frequency fluctuational conductivity. The dc case directly follows. Close to T_c the cutoff has no effect, and the known results for Gaussian fluctuations are recovered. Above T_c, and already for $\epsilon = \ln(T/T_c) > 10^{-2}$, we find strong suppression of the paraconductivity as compared to the Gaussian prediction, in particular in the real part of the paraconductivity. At high ϵ the cutoff effects are dominant. We discuss our results in comparison with data on high-T_c superconductors.

PACS. 74.40.+k Fluctuations (noise, chaos, nonequilibrium superconductivity, localization, etc.) – 74.20.De Phenomenological theories (two-fluid, Ginzburg-Landau, etc.) – 74.25.Nf Response to electromagnetic fields (nuclear magnetic resonance, surface impedance, etc.)

1 Introduction

After many years of studies of the fluctuational effects on various properties of superconductors, the discovery of high-T_c superconductors (HTC) has given new impulse to the study of fluctuational effects above the critical temperature T_c. In fact, high critical temperatures, short coherence lengths and strong anisotropy greatly enhance the temperature range of observation of fluctuational effects. This fact has led to the search for extensions of theoretical models, such as Ginzburg-Landau (GL) theory, to temperature ranges even well above T_c [1].

In general, fluctuational effects have been widely investigated in the past, both in conventional, low-T_c (LTC) superconductors [2] and in high-T_c cuprates (HTC). Among the various effects affected by thermal fluctuations, the dc excess conductivity above T_c has been experimentally studied most extensively [3–9]. Theoretical investigations dates from the sixties [2,10–13], and development of this topic proceeded until the discovery of HTCs. With some noticeable exception [1,3,5,14–17], the attention was always focussed in the temperature region close to the critical temperature. In that region, it is customary to discuss the data in terms of the Aslamazov-Larkin [10] (AL) and Maki-Thompson [12,18] contributions. Alternatively, the data are often described in terms of Gaussian fluctua-

tions, which by the simpler formalism of Ginzburg-Landau theory yield the same results as the microscopic AL approach [1,12] in clean superconductors.

While such treatments are in principle valid only close to T_c, in HTCs the range of observation of fluctuational effects is much wider. Thus, analysis of the data only in the strict proximity of T_c would miss a substantial amount of information, eventually leading to incomplete conclusions. Tools for investigating a wider temperature range are then not only interesting by themselves, but necessary for the study of HTC compounds.

Historically, it was recognized very early [19,20] that the experimental dc excess conductivity dropped much faster than predicted by, *e.g.*, AL theory [10], when temperature was raised above T_c. Early works [20,21] attributed this behavior to the unphysical contribution of high momentum modes to the fluctuation conductivity: close to T_c the uniform mode ($q = 0$) is the most diverging one, so that the contributions of the other modes are automatically negligible, but at even slightly higher temperatures this is no longer true, and one has to manage somehow the other contributions. An essentially similar framework, both in the experimental results and theoretical arguments, applied to the fluctuation diamagnetism above T_c [22–24]. In fact, the relevance of short or long wavelength modes is a rather general issue of the physics of phase transitions: it is here interesting to note that

[a] e-mail: silva@fis.uniroma3.it

arguments similar to those developed in this paper were raised, *e.g.*, in the treatment of the electrical resistivity in magnetic systems [25].

In most theoretical calculations a phenomenological approach was used: the dc excess conductivity was calculated within the time-dependent Ginzburg-Landau (TDGL) theory. Bearing in mind that within this approach slow variations of the order parameter (on the scale of ξ_0, the coherence length) are required [1,21], so that short-wavelength fluctuations are unphysical, a high-q cutoff was imposed [1,5,9,15–17,20,26–28]. A numerical approach was almost everywhere used, apart from a few analytical results in some special cases [9,15–17,28].

A second approach, grounded on microscopic calculations, was employed in early works to obtain the fluctuation diamagnetism [29–31]. The calculation of fluctuational conductivity was carried out by Varlamov and co-workers in several papers [32], within the Lawrence-Doniach (LD) model for layered superconductors (that in the high temperature range reduces to a collection of two-dimensional superconducting sheets). In this case the basis was the calculation of the full energy and momentum dependence of the fluctuation propagator and of the Green functions [14]. The dc conductivity was then calculated also for temperatures well above T_c.

Both these approaches gave as a result a strongly reduced dc excess conductivity well above T_c. A detailed comparison between the microscopic and the cutoffed, GL model for clean 2D superconductors has been given in reference [17], where it was shown that, with an appropriate choice of the cutoff, the two formulations gave the same temperature dependence of $\Delta\sigma$.

Comparisons with experiments were made on various materials: the phenomenological approach was successfully compared to data for the dc excess conductivity in amorphous alloys [20] and YBa$_2$Cu$_3$O$_{7-\delta}$ (YBCO) films [5,9] and crystals [33] within a three-dimensional model, and in Bi$_2$Sr$_2$CaCu$_2$O$_{8+x}$ (BSCCO) crystals [16,17] and tapes [34] with a two-dimensional expression. The 2D limit of the microscopic calculation [14] was shown to be in agreement with the data in BSCCO films [6]. In all cases the agreement extended at least up to $T \simeq 1.25T_c$. It is worth mentioning that a doping dependence of the cutoff number was found in BSCCO crystals [17], thus opening interesting issues about possible links between the phenomenological cutoff approach and microscopic properties.

In addition to the studies of the dc conductivity, a few papers appeared which dealt with the finite-frequency excess conductivity, mainly in the microwave range [26,27,35–39], together with the corresponding theoretical treatments [2,11,13,40]. In general, early experimental works [35] were found to agree reasonably well with pure Gaussian models [11], while the data in HTC showed a possible evidence for critical behavior close to T_c [37,38]. Differently from the dc case, only a very few preliminary works [26,27] explored the high temperature regime. In these cases, extra conductivity lower than the Gaussian expectation was experimentally found, but no

simple theoretical expressions were given. It is interesting to note that none of the reported microwave studies has shown evidence for the Maki-Thompson term, neither in low-T_c nor in high-T_c superconductors, as opposed to some dc experiments [2,41]. In addition, recent microscopic theoretical results have shown that in the ultraclean limit the fluctuationl conductivity is entirely given by the AL term, since the other contributions cancel out [42]. We find in these facts strong motivation for the present study.

It should be mentioned that the cutoff approach is still a debated topic [1,17,33]. However, it is a matter of fact that, to the lowest level, it gives a very good description of the data, while on fundamental grounds it is believed [1] to be a fundamental aspect of the GL theory.

In this paper we present an explicit calculation of the finite-frequency excess conductivity based upon the TDGL theory. We phenomenologically introduce the short wavelength cutoff in the fluctuational spectrum. Differently from previous results, we obtain closed forms for the dynamic excess conductivity. Formulae are presented for thin wires (one-dimensional systems, 1D), thin films (2D) and bulk (3D) superconductors. We explicitly include the in-plane anisotropy for the 2D case, and the three-axis anisotropy for the 3D case. Our results extend previous calculations in several ways: (i) to different dimensionalities, (ii) including the frequency dependence, (iii) giving explicit expressions for the cutoffed excess conductivity.

We discuss some of the features that can be expected in the experimental data when entering the short-wavelength regime. We expect that our calculations might be useful for the description of the frequency-dependent excess conductivity not too close to T_c.

2 Model

We use TDGL theory in order to investigate the main effects of a short-wavelength cutoff on the finite frequency conductivity. We work in absence of a dc magnetic field. We calculate the current response to a plane-wave electric field $\mathbf{E}e^{-i\omega t}$. Throughout the paper we use International System units for the ease of comparison of the results with the experiments. The GL functional is written in the general case as:

$$F = \int \mathrm{d}^D r \left[\sum_{j=1,..D} \frac{\hbar^2}{2m_j} \left| \left(\frac{\partial}{\partial r_j} - \frac{ie^\star}{\hbar} A_j \right) \psi\left(\mathbf{r}\right) \right|^2 \right.$$
$$\left. + \alpha \left| \psi\left(\mathbf{r}\right) \right|^2 + \frac{1}{2}\beta \left| \psi\left(\mathbf{r}\right) \right|^4 \right] \quad (1)$$

where the symbols have the following usual definitions:
- The vector potential $\mathbf{A} = -\frac{i}{\omega}\mathbf{E}$;
- $\alpha = a\epsilon$, where $\epsilon = \ln(T/T_c)$ is the reduced temperature [43];
- $e^\star = 2e$ is twice the electronic charge;
- m_j are the masses of the pair along the main crystallographic directions. Since we deal with the general case of anisotropic superconductors, all of them are in principle different.

The GL coherence lengths along the different axes are then defined as usual as $\xi_j = \hbar/\sqrt{2m_j\alpha}$. We are mainly interested in the behavior not too close to T_c, so that in the following we neglect the term $\sim \psi^4$ altogether (inclusion of this terms can be relevant very close to T_c [38,40,44]). Our aim is to calculate the longitudinal dynamical conductivity along the axis of application of the ac field, chosen to be the x axis. In the following we will consider three distinct "dimensionalities":

(i) 1D: thin superconducting wire, which we take to lay along the x axis. The section of the wire is assumed to be a square of side L, with $L < \xi_y, \xi_z$. Only m_x, ξ_x are relevant.

(ii) 2D: thin superconducting film, which is taken to lay in the x, y plane. The thickness $d < \xi_z$. Both m_x (ξ_x) and m_y (ξ_y) are relevant.

(iii) 3D: bulk anisotropic superconductor. The axes are taken along the crystallographic axes. All three masses and coherence lengths are relevant.

We do not rewrite all the preliminary calculations, that can be found elsewhere [38,40]. Instead, we sketch the path that has been followed. The time evolution of the order parameter, needed in order to calculate the dynamical conductivity, is determined by the TDGL equation describing relaxational dynamic for ψ, which is taken to include a white noise term. At this stage, the characteristic relaxation rate Γ_0 is introduced [45].

The response to the field $\mathbf{A}(t)$ is determined by the current operator averaged with respect to the noise (represented below by the brackets), and it can be expressed as a function of the correlation function of the order parameter $C(\mathbf{r}, t; \mathbf{r}', t') = \langle \psi(\mathbf{r}, t)\, \psi^\star(\mathbf{r}', t') \rangle$ at equal times:

$$\langle J_x(t) \rangle = -\frac{\hbar e^\star}{m_x} \int \frac{\mathrm{d}^D q}{(2\pi)^D} q_x C\left[\mathbf{k} = \mathbf{q} - \frac{e^\star}{\hbar}\mathbf{A}(t)\,; t, t\right] \tag{2}$$

where the momentum dependence has been shifted from $\mathbf{k}$ to the new vector $\mathbf{q} = \mathbf{k} + (e^\star/\hbar)\mathbf{A}(t)$.

The correlator has been calculated by, e.g., Dorsey [40] in the Gaussian approximation. We limit ourselves to the treatment of the linear response (we note however that the present approach has been used to calculate the non-linear excess conductivity close to T_c, Ref. [40]). Within the linear response, all the quadratic terms in the vector potential can be neglected, and the equal time correlator reads [46]:

$$C(\mathbf{q}; t, t) =$$

$$2k_B T \Gamma_0 \int\limits_0^{+\infty} \mathrm{d}s \exp\left\{ \left[-2\Gamma_0\alpha s - \Gamma_0\hbar^2 s \left(\frac{q_y^2}{m_y} + \frac{q_z^2}{m_z} \right) \right] \right.$$

$$\left. - \frac{\Gamma_0\hbar^2 s}{m_x}\left[q_x^2 - \frac{2e^\star q_x}{\hbar s} \int\limits_0^s \mathrm{d}u\, [A_x(t-u) - A_x(t)] \right] \right\} \cdot \tag{3}$$

The usual calculation is based on the integration of equation (2) for all momenta. Then, inserting equation (3) in

equation (2) and performing the integrals for the appropriate dimensionalities one gets the well known Gaussian results [11,40].

As discussed in the Introduction, we wish to phenomenologically extend the applicability range of the calculation to temperatures not too close to T_c, so that we explicitly discard the short-wavelength fluctuations by inserting a high-q cutoff in the integration of equation (2). There are several possible choices for this task. In the calculation of the dc conductivity with the aim of the Kubo formula, Gauzzi [15] has chosen a different cutoff for each q-component. Hopfengärtner et al. [5] have chosen, for the special case of YBCO taken as a uniaxial superconductor, the same cutoff for q_x and q_y, and a different one on q_z. Johnson et al. [20] used a cutoff on the modulus of q in order to describe results on 3D, isotropic superconductors.

It is worth stressing that in the comparison with the experiments, each cutoff becomes a new fitting parameter. It is in general important to reduce the number of such parameters, and particularly in a calculation like this, where phenomenological modifications are made. To meet this requirement, it is useful to note that on physical grounds the cutoff is measured in units of the inverse temperature-independent microscopic coherence length [21,47], ξ_0^{-1}. In homogeneous superconductors, even if anisotropic, there are no evident reasons for which a different number of ξ_0^{-1} should be used as a cutoff in different directions. We then introduce a single cutoff such that $\sqrt{\sum_{j=1,..D}[q_j\xi_j(0)]^2} < \Lambda$ in equation (2). We mention that this choice might be questionable when explicitly dealing with layered superconductors, where there is indeed a physical difference for in-plane and out-of-plane properties. This would require the use of the Lawrence-Doniach [48] or similar model, which is not the purpose of this work. A study limited to the dc conductivity can be found in references [5,28], while for a more general formulation of the extended (cutoffed) GL theory applied to layered superconductors we address the reader to a recent review [1].

To perform the calculations it is useful to manipulate the expression for the current using dimensionless variables:

$$k_j = q_j\xi_j, \text{ with } j = x, y, z, \text{ and}$$

$$w = \frac{\omega}{2\Gamma_0\alpha} = \omega\tau = \frac{\omega\tau_0}{\epsilon}$$

where in the latter relation the second equality defines the temperature-dependent GL characteristic time τ, and the third equality defines τ_0 [45]. In these units the cutoff is expressed as $K = \Lambda/\sqrt{\epsilon}$. The full expression for the current becomes:

$$\langle J_x(t) \rangle = -\frac{2e^\star k_B T}{\xi_x\xi_y\hbar} \int\limits_0^{+\infty} \mathrm{d}u e^{-u} \int \frac{\mathrm{d}^D k}{(2\pi)^D} k_x$$

$$\times \exp\left\{ uk^2 + B_x\frac{Ek_x}{w^2}\left[\mathrm{e}^{\mathrm{i}uw} - 1 - \mathrm{i}uw \right] \right\} \tag{4}$$

where $B_x = e^*(2\alpha^3 m_x)^{-\frac{1}{2}}/\Gamma_0$. This is the starting point for all the results presented in the following section. It is

intended that in 2D we make use of $\int \frac{\mathrm{d}^D q}{(2\pi)^D} \to \frac{1}{\mathrm{d}} \int \frac{\mathrm{d}^2 q}{(2\pi)^2}$, and in 1D $\int \frac{\mathrm{d}^D q}{(2\pi)^D} \to \frac{1}{L^2} \int \frac{\mathrm{d}q}{2\pi}$, that is we do not allow (consistently with the rest of the present work) high-q modes along the film thickness or wire section.

We do not explicitly report the long, but trivial procedures, for each specific case. In all cases we get, in the limit of small fields, the x-axis response written as:

$$\langle J_x \rangle = [\sigma'(\omega) + \mathrm{i}\sigma''(\omega)]\ E_x\ \mathrm{e}^{-\mathrm{i}\omega t} = \sigma(\omega) E_x\ \mathrm{e}^{-\mathrm{i}\omega t} \quad (5)$$

which defines the longitudinal complex conductivity $\sigma = \sigma' + \mathrm{i}\sigma''$. We recall that with the inclusion of all the momentum contributions, in 2D and 3D it was found [11,40] that the Gaussian conductivity was a scaling function of the frequency:

$$\sigma_g(\omega) = \sigma'_g(\omega) + \mathrm{i}\sigma''_g(\omega) = \sigma_g^{(\mathrm{dc})}\left[S_+\left(\omega\tau\right) + \mathrm{i}\,S_-\left(\omega\tau\right)\right] \quad (6)$$

where $S_+(x)$ and $S_-(x)$ are the scaling functions as can be found in reference [40] (with the subscript g we indicate the results obtained in the Gaussian approximation without a momentum cutoff), and they have the property that $S_+(x \to 0) = 1$ and $S_-(x \to 0) = 0$. The scaling expression has found some experimental confirmation in swept-frequency measurements in YBCO [37], but the temperature dependence of τ was found to markedly depart from the GL prediction, $\tau \sim \epsilon^{-1}$.

3 Results

In this section we present the resulting expressions for the finite-frequency excess conductivity for bulk superconductors, thin films and thin wires. In all cases, we find closed forms for the excess complex conductivity, which for compactness we leave in the form of functions of complex variable. Calculation of equation (4) leads to the following expression for the anisotropic 3D complex conductivity:

$$\sigma_{3D} = \frac{e^2}{32\hbar\xi_z(0)\epsilon^{1/2}}\frac{\xi_x(0)}{\xi_y(0)}\frac{16}{3\pi w^2}$$
$$\times \left\{ \mathrm{atn}\,K - (1-\mathrm{i}w)^{3/2}\ \mathrm{atn}\left(\frac{K}{\sqrt{1-\mathrm{i}w}}\right) \right.$$
$$\left. +\mathrm{i}w\left[\frac{K}{2\left(1+K^2\right)} - \frac{3}{2}\mathrm{atn}\,K\right] \right\}. \quad (7)$$

In anisotropic thin films we get:

$$\sigma_{2D} = \frac{e^2}{16\hbar\mathrm{d}\epsilon}\frac{\xi_x(0)}{\xi_y(0)}\left(-\frac{2}{w^2}\right)\left\{\left[\frac{1}{2}\ln\left(1+w^2\right) - w\mathrm{atn}w\right]\right.$$
$$+\mathrm{i}\left[w - \frac{w}{2}\ln\left(1+w^2\right) - \mathrm{atn}(w)\right]$$
$$-\left[\frac{1}{2}\ln\left(1+\frac{w^2}{(K^2+1)^2}\right) - w\mathrm{atn}\left(\frac{w}{K^2+1}\right)\right]$$
$$\left.-\mathrm{i}\left[\frac{w}{K^2+1} - \frac{w}{2}\ln\left(1+\frac{w^2}{(K^2+1)^2}\right) - \mathrm{atn}\left(\frac{w}{K^2+1}\right)\right]\right\} \quad (8)$$

and finally, in thin wires one has:

$$\sigma_{1D} = \frac{\pi}{16}\frac{e^2\xi_x(0)}{\hbar L^2\epsilon^{3/2}}\left(-\frac{16}{\pi w^2}\right)\left[\left(1-\frac{\mathrm{i}w}{2}\right)\mathrm{atn}\,(K)\right.$$
$$\left.+\frac{\mathrm{i}w}{2}\frac{K}{1+K^2} - \sqrt{1-\mathrm{i}w}\ \mathrm{atn}\left(\frac{K}{\sqrt{1-\mathrm{i}w}}\right)\right]. \quad (9)$$

Equations (7, 8, 9) are the main results of this paper.

A number of already known results can be obtained from these expressions as limiting cases: taking the limit for $K \to \infty$ and isotropic ξ's we recover the Schmidt's results [11] for the corresponding dimensionalities. Since $K = \Lambda/\epsilon^{\frac{1}{2}}$, the limit $K \to \infty$ contains either the no-cutoff (usual GL calculation), or the $T \to T_c$ limits. Correctly, close to the transition temperature the usual GL expressions are recovered.

As a by-product of equations (7, 8, 9), it is easy to obtain the dc excess conductivity for the various dimensionalities in the presence of a short-wavelength cutoff, taking the limit $\omega \to 0$. One gets:

$$\sigma_{3D}^{\mathrm{dc}} = \frac{e^2}{32\hbar\xi_z(0)\epsilon^{1/2}}\frac{\xi_x(0)}{\xi_y(0)}\frac{2}{\pi}\left[\mathrm{atn}\,K - K\frac{\frac{5}{3}K^2+1}{(K^2+1)^2}\right] \quad (10)$$

$$\sigma_{2D}^{\mathrm{dc}} = \frac{e^2}{16\hbar\mathrm{d}\epsilon}\frac{\xi_x(0)}{\xi_y(0)}\frac{1}{(1+K^{-2})^2} \quad (11)$$

$$\sigma_{1D}^{\mathrm{dc}} = \frac{e^2\xi_x(0)}{8\hbar L^2\epsilon^{3/2}}\left[\mathrm{atn}\,K - \frac{K\left(1-K^2\right)}{(K^2+1)^2}\right]. \quad (12)$$

Again, a number of already known results are obtained in the appropriate limits. In all cases, for $K \to \infty$ we get the usual results for the (anisotropic) Gaussian paraconductivity [2]. The cutoffed, 3D uniaxially isotropic result by Gauzzi [15] is recovered using $\xi_x = \xi_y$ in equation (10) and setting equal cutoffs in reference [15]. Similarly, we recover the known results in 2D [5,15,17] and 1D [28].

4 Discussion

There are several interesting features that emerge from the novel relations, equations (7, 8, 9) and the corresponding dc expressions. We first discuss shortly some peculiarities of the dc conductivity (Eqs. (10–12)) that seem to have been unnoticed in previous works.

A plot of the cutoff correction to the Gaussian paraconductivity, $\sigma^{\mathrm{dc}}(\epsilon; \Lambda, \omega = 0)/\sigma^{\mathrm{dc}}(\epsilon; \infty, \omega = 0)$, is reported in Figure 1 for $\Lambda = 0.74$ [47]. It is apparent that the correction is stronger for higher dimensionalities [49]. It is instructive to investigate the cases $K \to \infty$ (that is, the close vicinity of T_c) and $K \ll 1$ (that is, high reduced temperatures and/or strong cutoff effects). The latter case is more an oversimplification than a physically reachable limit, but it is very convenient in order to obtain analytical expressions. As can be derived from equations (10–12), in all the three cases one obtains the same temperature
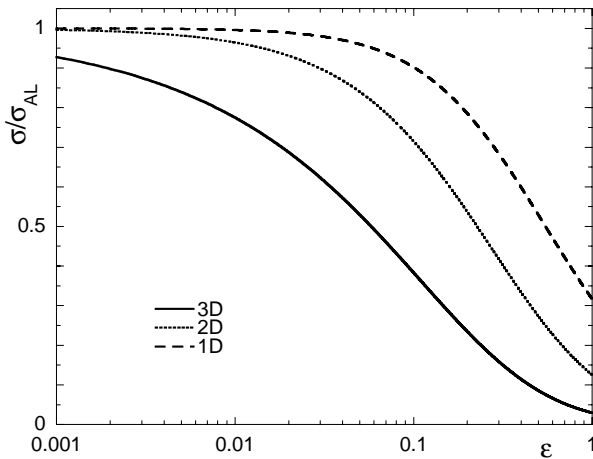
Fig. 1. Correction to the dc conductivity as a function of the reduced temperature $\epsilon = \ln T/T_c$, for cutoff number $\Lambda = 0.74$ [47], and for different dimensionalities.

dependence, namely:

$$\sigma^{dc}_{K \ll 1} = \frac{e^2}{\hbar} N_D \frac{1}{\epsilon^3} \qquad (13)$$

where $N_{1D} = \frac{1}{3}\frac{\xi_x(0)}{L^2}\Lambda^3$, $N_{2D} = \frac{1}{32}\frac{\xi_x(0)}{d\xi_y(0)}\Lambda^4$, $N_{3D} = \frac{1}{30\pi}\frac{\xi_x(0)}{\xi_y(0)\xi_z(0)}\Lambda^5$. The effect of the cutoff does change with the dimensionality (different powers of Λ), but only through a different prefactor, so that the determination of the dimensionality from the data at high ϵ should be carried on with care. In particular, it is tempting to identify the dimensionality from some power law of the excess conductivity with ϵ. This is surely not possible far from T_c, where the power law appears to be the same for all the dimensionalities. This fact could be somehow expected, since the introduction of the SWL cutoff introduces an additional length in the system, relevant far from the transition. Even a quantitative comparison, in the case e.g. of HTCS, might not allow for unambiguous identification of the dimensionality: taking as an example $\xi_x \simeq \xi_y$ and reasonable $\Lambda \sim 1$, one has to compare d with $\pi\xi_z(0)$. In the case of BSCCO, taking $d \simeq 3.3$ Å, the thickness of the double CuO layers, and $\xi_z(0) \simeq 1$ Å, the two prefactors are of the very same order of magnitude. In general, only a quantitative comparison in a wide temperature range can give indications on the effective dimensionality. We now turn to the discussion of the frequency dependence. We restrict this part of the discussion to the 2D and 3D cases, since we are not aware of experimental results for the dynamic conductivity in 1D systems. We discuss the temperature and frequency dependencies by means of the reduced variables $\epsilon = \ln(T/T_c)$ and $\omega\tau_o$. The use of $\omega\tau_0$ as a reduced variable does not require the exact determination of the GL relaxation time. However, for numerical estimates, assuming the BCS-derived value for Γ_0 one has $\omega\tau_0 \sim 10^{-3}$ for $\omega/2\pi = 10$ GHz: $\omega\tau_0 \ll 1$ even in the microwave region.

We employ the useful plots [5,28] of the conductivity normalized to the Gaussian (uncutoffed) results (note that
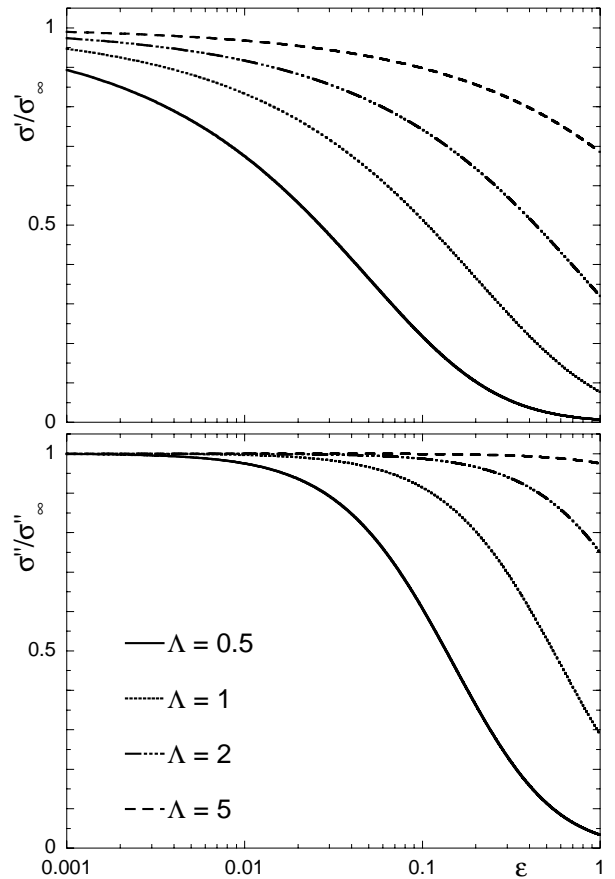

Fig. 2. Correction to the 3D dynamic conductivity vs. the reduced temperature ϵ, for $\omega\tau_0 = 10^{-3}$ and various cutoff numbers Λ. Upper panel: real part; lower panel: imaginary part. τ_0/ϵ is the Ginzburg-Landau relaxation time (see Sect. 2).

by using these plots the effects of the anisotropy cancel out).

In Figure 2 we plot the real and imaginary part of the conductivity normalized to the Gaussian values, $\sigma'(\omega, \epsilon, \Lambda)/\sigma'(\omega, \epsilon, \infty)$, and $\sigma''(\omega, \epsilon, \Lambda)/\sigma''(\omega, \epsilon, \infty)$, in the 3D case for various values of the cutoff number, Λ, as a function of the reduced temperature ϵ and $\omega\tau_0 = 10^{-3}$. As can be seen, the presence of a SWLC strongly depresses the dynamic conductivity at high ϵ. We note that the correction is much stronger on σ' than on σ''. For cutoff number $\Lambda = 1$ and $\epsilon = 10^{-1}$ the real part is reduced by $\sim 50\%$ with respect to the uncutoffed value, while the imaginary part remains at $\sim 90\%$ of the uncutoffed value. We also note that the effects of the cutoff are significant even at reduced $\epsilon \sim 10^{-2}$, that is almost in the full accessible temperature range, apart the small region very close to T_c (where, however, additional complications arise due to the possible entering of the critical region).

The frequency dependence is best studied with the plots at fixed ϵ and variable $\omega\tau_0$, as reported in Figure 3 for three reduced temperatures and $\Lambda = 1$. It is easy to notice that for all the ϵ depicted, the effect of the cutoff does not introduce a significant frequency dependence neither in σ', nor in σ'', up to very high frequencies (at the high
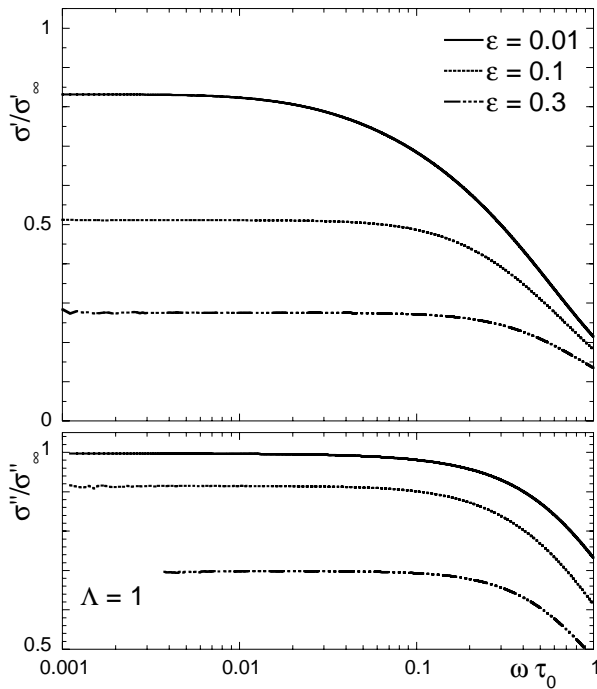
Fig. 3. Correction to the 3D dynamic conductivity *vs.* $\omega\tau_0$, with cutoff number $\Lambda = 1$. Upper panel: real part; lower panel: imaginary part.

Fig. 4. Correction to the 2D dynamic conductivity *vs.* the reduced temperature ϵ, for $\omega\tau_0 = 10^{-3}$ and various cutoff numbers Λ. Main panel: real part; inset: imaginary part.

Fig. 5. Correction to the 2D dynamic conductivity *vs.* $\omega\tau_0$, and cutoff number $\Lambda = 1$. Main panel: real part; inset: imaginary part.

edge of the microwave spectrum). The same figure shows again the larger effect of the cutoff on σ' than in σ''.

The fact that, for reasonable cutoff numbers and frequencies, the frequency dependence of the correction is nearly flat, while the temperature dependence changes with respect to the uncutoffed value, has a rather intriguing consequence: in fact, as recalled in Section 2, the Gaussian dynamic conductivity can be cast in a scaling form: $\sigma(\omega, \epsilon) = \sigma_{dc}(\epsilon)S(\omega\tau(\epsilon))$, where $\tau(\epsilon) = \tau_0/\epsilon$ in the Gaussian regime. Our present results still predict an *approximate* scaling, but the temperature dependence of τ is apparently different from the uncutoffed result [50]. The exact scaling prediction [40] is reinstated for infinite cutoff. It would be interesting to perform wideband measurements in an extended temperature range above T_c in view of this novel feature of the theoretical expressions.

Essentially the same features, but with a less pronounced effect of the cutoff are exhibited by 2D systems, as shown by Figures 4 and 5. We then expect that in strongly layered systems the frequency dependence of the dynamic paraconductivity is essentially unaffected by the cutoff in a reasonably wide temperature range (up to $\epsilon \sim 0.2$), while effects of the cutoff should be easier to observe in measurements of the real part of the paraconductivity at fixed frequencies and variable ϵ.

We now discuss our results in comparison with experimental data for the microwave excess conductivity in high-T_c superconductors. It should be noted that most of the microwave data, where one might observe some significant effect of the frequency, were devoted to studies well inside the superconducting state or, at most, of the crit-
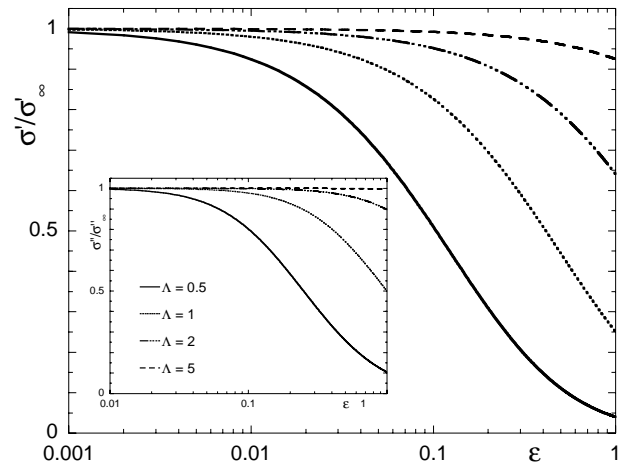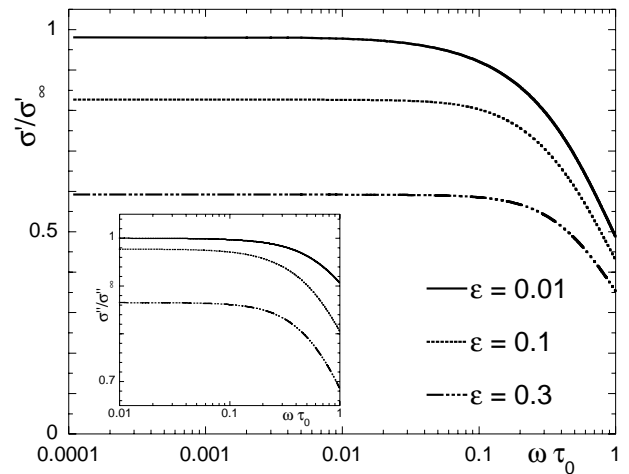
ical regime very close to T_c. As a consequence, there are nearly no published data (to our knowledge) of the finite-frequency excess conductivity, in temperature ranges extended enough above T_c. In order to assess the question whether or not our cutoff approach describes the correct trend in the observations, we consider the data for the complex excess conductivity above T_c taken in Zn-doped YBCO crystals [39]. In this case, a Ginzburg-Landau-like analysis suggested that the compound behaves nearly as a 2D system [39], but the overall magnitude of the excess conductivity was about half of the theoretical prediction when the cell unit (≈ 11.7 Å) was taken as effective layer separation. In Figure 6 we plot the measured complex excess conductivity at 25 and 36 GHz (as digitized from Ref. [39]), the 2D GL prediction ($\Lambda = \infty$) at 36 GHz and the 2D, cutoffed curve at the two frequencies for $\Lambda = 0.247$ (that is [47], a momentum cutoff of $(3\xi_0)^{-1}$). The result is encouraging: in particular, a nearly quantitative fit is obtained not too close to T_c
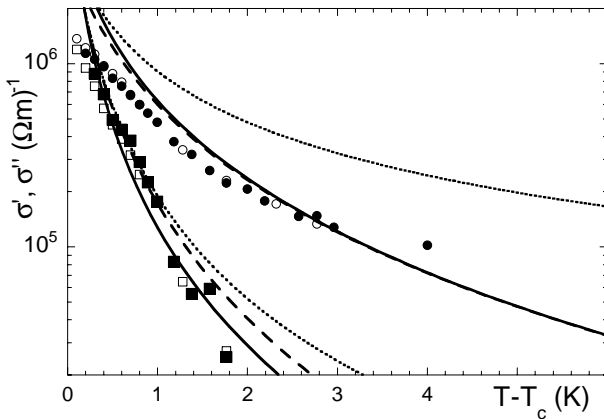
Fig. 6. Data for the dynamic conductivity of Zn-doped YBCO, from reference [39], at 25 GHz (open symbols) and 36 GHz (full symbols). Circles: real part. Squares: imaginary part. Dotted lines: fits with the uncutoffed expression, $\omega\tau_0 = 0.0086$, corresponding to 36 GHz. Dashed lines: 2D expression, equation (8), with cutoff number $\Lambda = 0.247$ (see text), $\omega\tau_0 = 0.0086$. Continuous lines: 2D expression, equation (8), with $\Lambda = 0.247$ (see text), $\omega\tau_0 = 0.006$. The momentum cutoff better describes the experimental trends than the plain GL expression.

(we do not discuss the possible occurence of a dimensional crossover approaching T_c), without adjusting the other parameters [51], thus demonstrating that the proposed extension of the GL theory can correctly describe the features experimentally observed. New measurements, in extended temperature ranges above T_c, would be extremely useful to check the applicability of the momentum-cutoff scenario.

5 Conclusions

In conclusion, we have performed a Ginzburg-Landau calculation of the dynamic conductivity in anisotropic bulk, thin films and thin wires superconductors. According to the general prescriptions of the GL theory [1,21], we have introduced a short-wavelength cutoff in the spectrum of the accessible momenta. We have derived closed forms for the dynamic conductivity in the three cases abovementioned, that can be directly used for data fitting. We have predicted peculiar behaviors of the complex conductivity as the short-wavelength regime shows up. The analysis of some of the existing data for the finite-frequency conductivity finds a description in terms of the model here presented. More data are required to discuss the details of the excess conductivity at microwave frequencies.

Appendix: Additional remarks: The total-energy cutoff

It is a recently debated topic whether the momentum cutoff here adopted should be or not replaced by a cutoff in the total energy of the pair [1,33]. In the 3D energy cutoff scenario, the number Λ should be replaced by $\sqrt{c^2 - \epsilon}$, with c a new cutoff number, so that momentum-cutoff expressions can be easily rewritten in terms of energy cutoff (for a discussion, we address the reader to the review, Ref. [1]). Measurements of the dc conductivity showed a quite good agreement with the momentum cutoff scenario in BSCCO crystals [16,17], and with the energy cutoff in YBCO crystals [33]. Analysis of the finite-frequency conductivity at high reduced temperatures might help to resolve this issue.

References

1. T. Mishonov, E. Penev, Int. J. Mod. Phys B **14**, 3831 (2001)
2. W.J. Skocpol, M. Tinkham, Rep. Prog. Phys. **38**, 1049 (1975)
3. P.P. Freitas, C.C. Tsuei, T.S. Plaskett, Phys. Rev. B **36**, 833 (1987)
4. M. Ausloos, Ch. Laurent, Phys. Rev. B **37**, 611 (1988)
5. R. Hopfengartner, B. Hensel, G. Saemann-Ischenko, Phys. Rev. B **44**, 741 (1991)
6. G. Balestrino, M. Marinelli, E. Milani, Phys. Rev. B **46**, 14919 (1992)
7. S. Labdi, S. Megtert, H. Raffy, Solid State Commun. **85**, 491 (1993)
8. V. Calzona, M.R. Cimberle, C. Ferdeghini, G. Grasso, D.V. Livanov, D. Marré, M. Putti, A.S. Siri, G. Balestrino, E. Milani, Solid State Commun. **87**, 397 (1993)
9. A. Gauzzi, D. Pavuna, Phys. Rev. B **51**, 15420 (1995)
10. L.G. Aslamazov, A.I. Larkin, Soviet Phys. Solid State **10**, 875 (1968) [Fiz. Tverd. Tela (Leningrad) **10**, 1104 (1968)]; Phys. Lett. A **26**, 238 (1968)
11. H. Schmidt, Z. Phys **216**, 336 (1968); *ibidem* **232**, 443 (1970)
12. K. Maki, Prog. Theor. Phys. **39**, 897 (1968); *ibidem* **40**, 193 (1968)
13. R.A. Klemm, J. Low Temp. Phys. **16**, 381 (1974)
14. L. Reggiani, R. Vaglio, A.A. Varlamov, Phys. Rev. B **44**, 9541 (1991)
15. A. Gauzzi, Europhys. Lett. **21**, 207 (1993)
16. E. Silva, D. Neri, M. Esposito, R. Fastampa, M. Giura, S. Sarti, Physica C **341-348**, 1927 (2000)
17. E. Silva, S. Sarti, R. Fastampa, M. Giura, Phys. Rev. B **64**, 144508 (2001)
18. R.S. Thompson, Phys. Rev. B **1**, 327 (1970)
19. W.L. Johnson, C.C. Tsuei, Phys. Rev. B **13**, 4827 (1976)
20. W.L. Johnson, C.C. Tsuei, P. Chaudhari, Phys. Rev. B **17**, 2884 (1978)
21. N.R. Werthamer, in Superconductivity, edited by R.D. Parks (Marcel Dekker, New York, 1969)
22. B.R. Patton, V. Ambegaokar, J. Wilkins, Solid State Comm. **7**, 1287 (1969)
23. J.P. Gollub, M.R. Beasley, M. Tinkham, Phys. Rev. Lett. **25**, 1646 (1970)

24. J.P. Gollub, M.R. Beasley, R. Callarotti, M. Tinkham, Phys. Rev. B **7**, 3039 (1973)
25. see, *e.g.*, M.E. Fisher, J.S. Langer, Phys. Rev. Lett. **20**, 665 (1968); D.J.W. Geldart, T.G. Richard, Phys. Rev. B **12**, 5175 (1975); M. Ausloos, K. Durczewski, Phys. Rev. B **22**, 2439 (1980); and references therein
26. D. Neri, R. Marcon, E. Silva, R. Fastampa, L. Iacobucci, S. Sarti, Int. J. Mod. Phys. B **13**, 1097 (1999)
27. D. Neri, R. Fastampa, M. Giura, R. Marcon, S. Sarti, E. Silva, J. Low Temp. Phys. **117**, 1099 (1999)
28. M.W. Coffey, preprint (2001)
29. K. Maki, H.Takayama, J. Low Temp. Phys. **5**, 313 (1971)
30. J. Kurkijarvi, V. Ambegaokar, G. Eilemberger, Phys. Rev. B **5**, 868 (1972)
31. R.R. Gerhardts, Phys. Rev. B **9**, 2945 (1974)
32. A.A. Varlamov, G. Balestrino, E. Milani, D.V. Livanov, Adv. in Phys. **48**, 655 (1999)
33. C. Carballeira, S.R. Currás, J. Vina, J.A. Veira, M.V. Ramallo, F. Vidal, Phys. Rev. B **63**, 144515 (2001)
34. Q. Wang, G.A. Saunders, H.J. Liu, M.S. Acres, D.P. Almond, Phys. Rev. B **55**, 8529 (1997)
35. R.V. D'Aiello, S.J. Freedman, Phys. Rev. Lett. **22**, 515 (1969); S.L. Lehoczky, C.V. Briscoe Phys. Rev. Lett. **23**, 695 (1969); Phys. Rev. B **4**, 3938 (1971)
36. S.M. Anlage, J. Mao, J.C. Booth, D.H. Wu, J.L. Peng Phys. Rev. B **53**, 2792 (1996)
37. J.C. Booth, D.H. Wu, S.B. Qadri, E.F. Skelton, M.S. Osofsky, A. Piqué, S.M. Anlage, Phys. Rev. Lett. **77**, 4438 (1996)
38. D. Neri, E. Silva, S. Sarti, R. Marcon, M. Giura, R. Fastampa, N. Sparvieri, Phys. Rev. B **58**, 14581 (1998)
39. J.R. Waldram, D.M. Broun, D.C. Morgan, R. Ormeno, A. Porch, Phys. Rev. B **59**, 1528 (1999)
40. A.T. Dorsey, Phys. Rev. B **43**, 7575 (1991)
41. M. Ausloos, F. Gillet, Ch. Laurent, P. Clippe Z. Phys. B **84**, 13 (1991)
42. D.V. Livanov, G. Savona, A.A. Varlamov, Phys. Rev. B **62**, 8675 (2000)
43. L.P. Gor'kov, Zh. Eksp. Teor. Fiz. **36**, 1918 (1959) [Soviet Phys. JETP **9**, 1364 (1959)]
44. H.-J. Mikeska, H. Schmidt, Z. Physik **230**, 239 (1970)
45. In BCS superconductors one finds [2], from comparison with microscopic theory, $\Gamma_0 = (8k_B T/\hbar\pi a)$, where k_B is the Boltzmann constant. In exotic superconductors the value of Γ_0 may be numerically different. This aspect has been clearly discussed in reference [1]. The qualitative results here presented do not depend on the precise numerical value of Γ_0
46. The convergence of the integral written in this form is assured when expansion for small fields is made in the subsequent steps of the calculation. The full expression is obviously convergent, see equation (4) in reference [38]. We thank T. Mishonov for bringing our attention to this point
47. For the sake of compactness, throughout the paper we use only the GL zero-temperature coherence length, $\xi(0)$, instead of the microscopic coherence length $\xi_0 = \xi(0)/0.74$. As a consequence, the cutoff $\Lambda = 0.74$ means a momentum cutoff $Q = \xi_0^{-1}$
48. W.E. Lawrence, S. Doniach, in Proceedings of the 12th International Conference on Low Temperature Physics, edited by E. Kanda (Kiegaku, Tokio, 1971)
49. As pointed out by other authors [5,9,15,28], this behaviour can easily mimic the appearance of dimensional crossovers
50. In fact, it is easy to derive an approximate expression for σ with $w \ll 1$, from which both the extremely slow frequency dependence and the new approximate scaling are exploited
51. A scale factor would substantially improve the fit, at the expense of the introduction of an additional free parameter. Purpose of the present comparison with the data is to show that the proposed extension to the GL theory is in agreement with the experimental trends